Detection of coherent acoustic phonons by time-resolved second-harmonic generation

H. B. Zhao,[1,2,*] Y. Fan,[1] G. Lüpke,[1] A. T. Hanbicki,[3] C. H. Li,[3] and B. T. Jonker[3]
[1]*Department of Applied Science, College of William & Mary, Williamsburg, VA 23185, USA*
[2]*Department of Optical Science and Engineering, Key Laboratory of Micro and Nano Photonic Structures (Ministry of Education), Fudan University, Shanghai 200433, P. R. China*
[3]*Naval Research Laboratory, Washington, DC 20375, USA*
(Received 18 February 2011; revised manuscript received 10 April 2011; published 28 June 2011)

We report on observation of coherent longitudinal acoustic phonons in Fe/AlGaAs (001) heterostructure by time-resolved second-harmonic generation (TRSHG). The phonon induces not only a fast and highly damped oscillatory signal but also a long-lived one that exhibits an oscillating period identical to that obtained from the reflectivity measurement. The long-lived oscillatory second-harmonic generation is generated by an electric field modulated at 42.5 GHz because of the interference of the incident beam and the reflected light by the propagating phonon. TRSHG lets us probe the internal field modulated by phonons and differentiate their impacts at the interface and in the bulk.

DOI: 10.1103/PhysRevB.83.212302 PACS number(s): 78.20.hb, 42.65.Ky

I. INTRODUCTION

Coherent acoustic phonons have been generated and detected by the pump-probe technique using ultrafast laser pulses in semiconductor systems,[1–6] particularly in heterostructures with a thin metallic capping layer on the top.[7–11] The capping layer acts to absorb an intense pump laser pulse, launching a strain wave consisting of coherent phonons into the layer underneath. The phonons then propagate at the speed of sound through the medium, leading to long-lived oscillations in the reflectance of the time-delayed probe pulse if the medium is transparent for the probe light.

The period of the oscillations can be described by $T = \lambda/2nV\cos\theta$ (Eq. 1), with probe wavelength λ, refractive index n, and sound velocity V and where $\sin\theta = (1/n)\sin\theta_{\text{probe}}$, with an angle of incidence θ_{probe}.[1,5,11] The linear dependence of the oscillation period on λ can be explained by the interference of the light beams reflected from the sample surface, heterointerface, and propagating phonon pulse.[1,5,11] The light reflected by the phonon wave travels a distance of $2nVt/\cos\theta$ in the medium, leading to a phase shift $4\pi nVt\cos\theta/\lambda$, proportional to the delay time t, with respect to the light reflected by the surface and the interface. Thus, a periodic oscillating intensity is generated for the overall reflection. Another possibility is that the probe photon scatters exclusively on the wavelength-matched phonons through the backward Raman scattering.[2,7,11–13] The Raman scattering provides the λ filter via the momentum selection rule $q = 2nk\cos\theta$, with phonon wave vector q and probe beam wave vector k. Both scenarios provide the same formula for the dependence of T on λ. They also require small enough or no absorption of the probe light by the semiconductor to detect the phonons deeply propagating into the bulk. The phonon-induced long-lived oscillatory signals otherwise would be strongly damped because of light absorption. Furthermore, in the conventional one- or two-color pump-probe measurements, the probe beam may reflect the direct interaction of light with localized phonon, but the detection of the electric fields throughout the medium modulated by the phonon is not easily achievable.

In this paper we investigate the photogenerated acoustic phonon by time-resolved second-harmonic generation (TRSHG) in Fe/AlGaAs heterostructures on GaAs substrates. The TRSHG spectra show not only oscillations at a frequency of ∼115 GHz, which can be described by the aforementioned formula, but also oscillations at a frequency of 42.5 GHz, identical to that observed in the time-resolved reflectivity measurement. Our results clearly indicate oscillating electric field strength near the interface of the heterostructure as a result of interference of the incident probe beam and its reflection by the acoustic phonon. This self-modulated interference pattern generates the oscillations at 42.5 GHz in the TRSHG spectra. TRSHG also allows us to separately identify the impacts induced by phonons at the interface and in the bulk.

II. EXPERIMENTAL PROCEDURE

The samples were grown by molecular-beam epitaxy. The semiconductor heterostructure consists of an n-$Al_{0.1}Ga_{0.9}As$ (AlGaAs) epilayer (∼850 Å) on an n-type GaAs (001) substrate. A 100-Å-thick Fe (001) film was grown on top of AlGaAs at 10–15 °C to minimize potential intermixing. The details of the samples can be found elsewhere.[14]

The TRSHG measurements were performed with a Ti:Sapphire amplifier delivering 150 fs pulses at 800 nm and a 1-KHz repetition rate. A modulated pump beam with 40-μJ pulse energy is focused to a spot ∼1.5 mm in diameter on the sample mounted on a computer-controlled rotation stage. A p-polarized probe beam with 20-μJ pulse energy is incident on the sample at $\theta_{\text{probe}} = 45°$, with the beam diameter slightly smaller than that of the pump beam. A mechanical motorized translation stage is used to vary the time delay between the pump and the probe beams, and the time resolution is only limited by the laser pulse width. The reflected second-harmonic generation (SHG) signal passes through an analyzer and is detected with high signal-to-noise ratio using a photomultiplier tube and a chopper, in combination with a lock-in amplifier. A prism and color glass filters are used to separate the SHG beam from the fundamental laser beam. For time-resolved reflectivity measurements, the reflected probe beam is detected by a silicon photodiode. The schematics of the experimental geometry and sample structure are shown in

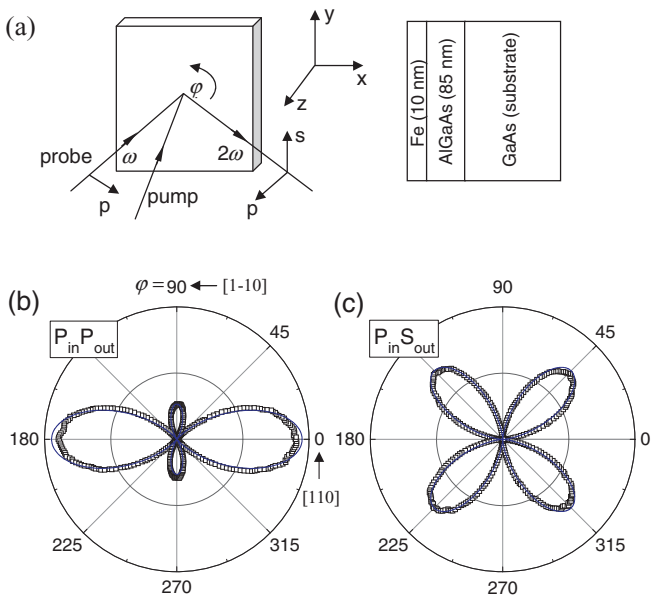

FIG. 1. (Color online) (a) Schematics of the experimental geometry and sample structure. Azimuthal dependence of (b) *p*-polarized and (c) *s*-polarized SHG, with the *p*-polarized incident light in Fe/AlGaAs (001). The directions along 0° and 90° correspond to the [110] and [1–10] axes, respectively, in the bulk GaAs. The solid curves are the best fits to the measured SHG intensity.

Fig. 1(a) where φ denotes the rotation angle and we define $\varphi = 0^\circ$ when [110] is oriented along the x axis.

III. EXPERIMENTAL RESULTS AND DISCUSSION

Figures 1(b) and 1(c) show the rotational SHG intensity without a pump beam for combinations of *p*-polarized incident light with *p*-polarized SHG ($P_{\text{in}}P_{\text{out}}$) and with *s*-polarized SHG ($P_{\text{in}}S_{\text{out}}$). The *s*-polarized SHG shows fourfold symmetry, indicating a pure bulk response from the AlGaAs layer and the substrate. Both four- and twofold symmetries are observed for *p*-polarized SHG. This is caused by a superposition of bulk SHG response from AlGaAs, which has the form $E_b \cos(2\varphi)$, and an isotropic component E_i generated at the Fe/AlGaAs interface.[15] The surface contribution to isotropic SHG is small because of oxidization with exposure to ambient air. Thus, total SHG intensity is given by $I = |E_b \cos(2\varphi) + E_i|^2$. We obtain a ratio of 1:3.3 between E_i and E_b from the best fit to the SHG intensity shown in Fig. 1(b). This ratio is much larger than that obtained from the pure GaAs substrate or AlGaAs/GaAs heterostructure,[16] indicating a pronounced interface contribution to SHG from Fe. We find from Fig. 1(b) that total SHG becomes zero at $\varphi = 54^\circ$, where the interface and bulk responses cancel each other out.

Figure 2 shows TRSHG measurements at $\varphi = 0^\circ$ and $\varphi = 90^\circ$, marked by arrows in Fig. 1(b), which correspond to the [110] and [1-10] axes, respectively. For both measurements, a highly damped oscillatory signal lasts ~30 ps [Figs. 2(b) and 2(e)] and long-lived oscillations persist longer than 1 ns with extremely small damping, as shown in Figs. 2(c) and 2(f), where exponential decaying parts are subtracted from raw data in Figs. 2(a) and 2(d). Apart from the oscillatory signals, TRSHG for [110] shows a slowly decaying positive

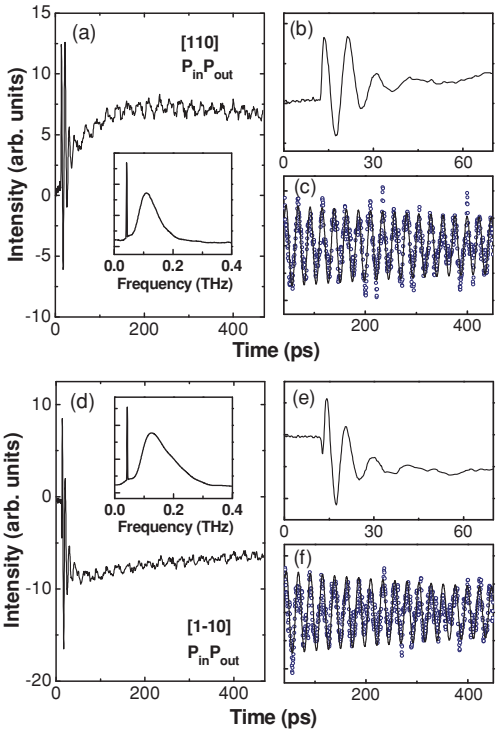

FIG. 2. (Color online) Pump beam-induced transient *p*-polarized SHG intensity along the (a–c) [110] and (d–f) [1–10] directions with *p*-polarized incident light. The solid curves in (c) and (f) are fits to the long-lived oscillatory signals, shown by open circles, which are subtracted by exponential decaying values from raw data. The insets in (a) and (d) show the Fourier spectra after removing the background. Both spectra show two peaks centered at 42.5 and 115 GHz.

direct current (dc) component, whereas the response of [1–10] is negative. The bulk response E_b is at least three times larger than E_i at the interface, and both components are in phase ($I = |E_b + E_i|^2$) for the [110] axis but out of phase ($I = |E_b - E_i|^2$) for the [1–10] axis. The change of E_b by pump modulation leads to the same modulations of total SHG intensity I for both directions, whereas the change of E_i results in opposite signals. Therefore, the sign change of the dc components between [110] and [1–10] axes must be caused by a strong modulation of interfacial response. On the contrary, the change of the bulk response is relatively weak.

This slowly exponential decaying component also appears in *p*-polarized TRSHG obtained for the [100] axis, as shown in Fig. 3(a). In such a measurement, only the interface response contributes to the SHG signal. In contrast, this component is extremely small for *s*-polarized SHG [Fig. 3(c)], which is generated only from the bulk. We therefore conclude that the dc signal slowly decays mainly because of the interface response. We believe that this signal is mainly caused by the heating effect that results from incoherent phonons, because a small negative component is still observable even before the zero time overlap, ~1 ms, in TRSHG for [1–10], whereas it is positive for [110]. The signal of *s*-polarized SHG before the zero time overlap for [100] is nearly zero, revealing that the heating effect is significantly weaker in the bulk at such a long time scale.

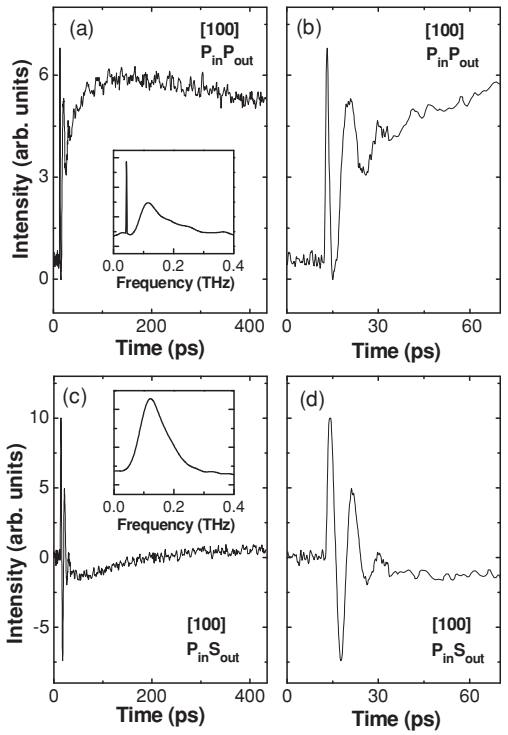

FIG. 3. Pump beam-induced transient (a, b) *p*-polarized and (c, d) *s*-polarized SHG intensity along the [100] direction with *p*-polarized incident light. The insets in (a) and (c) show the Fourier spectra after removing the background. The spectra in (a) show two peaks centered at 42.5 and 115 GHz, whereas only one peak centered at 115 GHz is present in (c).

We now turn to the oscillatory part in TRSHG. As shown in the insets of Fig. 2, the Fourier power spectrum has two peaks centered at frequencies of 42.5 GHz and 115 GHz, corresponding to the long-lived and highly damped oscillations, respectively. The higher-frequency mode can be assigned to a coherent longitudinal acoustic (LA) phonon propagating into the AlGaAs layer and the substrate.[8,17] The acoustic phonon resonance in the thin Fe film may not account for this mode, because such resonance is expected to oscillate at ~260 GHz or higher as given by $f = m\sqrt{C_{33}/\rho}/2d$, where C_{33} and ρ are the out-of-plane elastic constant and the mass density of the Fe film, respectively; m denotes the mode index number; and d is the film thickness.[18,19] We then determine the sound velocity of $\sim 5.0 \times 10^3$ m/s in AlGaAs using Eq. 1 and with the following parameters: $\lambda = 400$ nm, $n = 4.6$, and $T = 8.7$ ps. This velocity is close to the value in GaAs obtained in a time-resolved reflectivity measurement, which is discussed later, and it is in agreement with the velocity of the LA phonon reported previously.[6,12,20] For the [110] and [1–10] axes, this fast oscillatory component exhibits a nearly identical phase, pointing to the dominant bulk contribution. The phase of *s*-polarized TRSHG for [100] is the same as that of [110] and [1–10], whereas a small phase shift is observed between oscillatory *p*- and *s*-polarized TRSHG for the [100] axis, as shown in Figs. 3(b) and 3(d). This phase shift is correlated with the depth where SHG occurs; i.e., the *p*-polarized signal is generated at the interface, whereas the *s*-polarized signal is from the bulk.

For either of the two aforementioned detection mechanisms, the SHG beam has to propagate into the medium and interact directly with the phonon wave. Because the energy of SHG (3.1 eV) is significantly higher than that of the band gap of the AlGaAs layer and the GaAs substrate, it is strongly attenuated when propagating deeply into the sample. Thus, the oscillatory SHG signal at a frequency of 115 GHz is highly damped, with a decay time of ~15 ps. Within this decay time, the phonons travel a distance of ~70 nm in the medium, and this distance is approximately on the same order as the optical absorption length α^{-1} for the SHG light (~20 nm). The longer duration time may result from the finite width of the phonon waves, which extends on the tens of nanometers scale, considering the thermoelastic model and the bouncing strain pulse caused by acoustic impedance mismatch of the Fe film to the substrate.[1] The consecutive fast oscillations have slightly different periods. This can be attributed to the gradual change of doping concentration in the AlGaAs layer of the Schottky junction,[14] which may alter the sound velocity and the index of refraction.

The long-lived oscillations at a frequency of 42.5 GHz in TRSHG are not caused by direct interaction between SHG and phonon wave because of the limited penetration depth of SHG light. However, the period of the oscillations is the same as that of the oscillatory signal obtained from the time-resolved reflectivity measurements shown in Fig. 4. In the reflectivity measurement, the probe beam may propagate deeply into the GaAs substrate, be reflected or scattered backward by the phonon, and then travel back to the sample surface without significant absorption; thus, we can see the long-lived oscillations with weak damping. From the reflectivity measurements, we determine the sound velocity of 4.8×10^3 m/s in GaAs using Eq. 1 and the following parameters: $\lambda = 800$ nm, $n = 3.65$, and $T = 23.5$ ps.

The leading edge of the light reflected by phonons may interfere with the trailing edge of the incident light in the heterostructure, because the 150-fs light pulse may extend >10 μm in the medium. Thus, spatiotemporal oscillatory electric field intensity with frequency $f = 42.5$ GHz is generated over a distance stretching from the heterointerface to the depth that the phonon wave has reached. This modulated electric field generates the long-lived oscillating SHG signal,

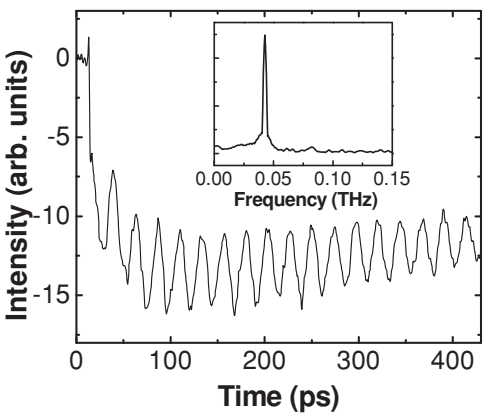

FIG. 4. Pump beam-induced transient reflectivity spectrum. The inset shows the Fourier spectrum with a peak centered at 42.5 GHz.

which is reflected in our TRSHG spectra. The ratio for the amplitude of the long-lived oscillating SHG versus the total SHG yield is on the order of 10^{-3}, which is $\sim 1/3$ of the reflectivity modulation (Fig. 4). This significant long-lived SHG modulation is reasonable, because the SHG yield is quadratic to the total electric field; thus, its modulation depth is linearly proportional to the field intensity of the probe light reflected by the phonon waves.

Only a small phase difference ($\sim 10^{\circ}$) of the oscillatory components occurred between [110] and [1–10] orientations [Figs. 2(c) and 2(f)], in contrast to the sign change, i.e., 180°, of the dc components. Therefore, the bulk contribution to the oscillatory component is dominant compared to that from the interface. In Fig. 3(a), where the *p*-polarized SHG signal only originates from the interface, such an oscillatory component is also present, but it has a smaller amplitude. However, its phase is close to that of the bulk, indicating that oscillatory SHG from the bulk originates mainly from the layers not far from the interface; otherwise, the phase may have a significant shift, because the overall field intensity is spatially modulated at a length ($d \approx 110\,nm$) equal to half the wavelength in (Al)GaAs. Considering that the absorption length of SHG light is much smaller than d, we may expect the phase shift to be small.

The *s*-polarized TRSHG for the [100] axis does not show the slow oscillatory component [Fig. 3(c)]. This can be explained by the afore-discussed field modulation. The intensity of *s*-polarized SHG is described by $E_y(2\omega) \propto \chi_{yzx} E_z(\omega) E_x(\omega)$, where χ_{yzx} is the second order nonlinear susceptibility and $E_z(\omega)$ and $E_x(\omega)$ are the electric fields in the z and x directions, respectively. However, the phases of these two field components are opposite upon reflection by the acoustic wave, leading to a 180° shift in interference patterns between $E_z(\omega)$ and $E_x(\omega)$. Therefore, $E_z(\omega)E_x(\omega)$ is nearly constant to the first order, and no oscillatory SHG signal can be detected. For other measurements, $E_x^2(\omega)$ may contribute to SHG and thus give rise to the oscillations. The Raman scattering cannot account for the observed polarization dependence of the SHG oscillations.

IV. CONCLUSION

In this paper we presented generation and detection of coherent phonon spectroscopy in Fe/AlGaAs Schottky structures by TRSHG. The phonons induce long-lived oscillations with a frequency of 42.5 GHz, identical to that obtained from the time-resolved reflectivity measurement, as well as a fast, strongly damped oscillatory signal with a frequency of $\sim$115 GHz. The long-lived SHG component is generated by the periodic modulation of the electric field intensity because of the propagating acoustic waves in the medium. The phase sensitivity of TRSHG enables us to differentiate the effect induced by phonons at the interface and in the bulk.

ACKNOWLEDGMENTS

This work was sponsored in part by the Office of Naval Research, National Natural Science Foundation of China (Grants No. 60908005 and No. 11074044), Shanghai Pujiang Program, and Okawa Foundation.

*hbzhao@fudan.edu.cn

[1] C. Thomsen, H. T. Grahn, H. J. Maris, and J. Tauc, Phys. Rev. B **34**, 4129 (1986).
[2] R. Merlin, Solid State Commun. **102**, 207 (1997).
[3] O. Matsuda, T. Tachizaki, T. Fukui, J. J. Baumberg, and O. B. Wright, Phys. Rev. B **71**, 115330 (2005).
[4] C.-K. Sun, J. -C. Liang, and X. -Y. Yu, Phys. Rev. Lett. **84**, 179 (2000).
[5] S. Wu, P. Geiser, J. Jun, J. Karpinski, and R. Sobolewski, Phys. Rev. B **76**, 085210 (2007).
[6] A. Steigerwald, Y. Xu, J. Qi, J. Gregory, X. Liu, J. K. Furdyna, K. Varga, A. B. Hmelo, G. Lüpke, L. C. Feldman, and N. Tolk, Appl. Phys. Lett. **94**, 111910 (2009).
[7] I. Bozovic, M. Schneider, Y. Xu, R. Sobolewski, Y. H. Ren, G. Lüpke, J. Demsar, A. J. Taylor, and M. Onellion, Phys. Rev. B **69**, 132503 (2004).
[8] Y. -M. Chang, Appl. Phys. Lett. **82**, 1781 (2003).
[9] T. Berstermann, C. Brüggemann, M. Bombeck, A. V. Akimov, D. R. Yakovlev, C. Kruse, D. Hommel, and M. Bayer, Phys. Rev. B **81**, 085316 (2010).
[10] A. Huynh, B. Perrin, N. D. Lanzillotti-Kimura, B. Jusserand, A. Fainstein, and A. Lemaître, Phys. Rev. B **78**, 233302 (2008).
[11] Y. Ezzahri, S. Grauby, J. M. Rampnoux, H. Michel, G. Pernot, W. Claeys, S. Dilhaire, C. Rossignol, G. Zeng, and A. Shakouri, Phys. Rev. B **75**, 195309 (2007).
[12] K. Mizoguchi, M. Hase, S. Nakashima, and M. Nakayama, Phys. Rev. B **60**, 8262 (1999).
[13] N. D. Lanzillotti-Kimura, A. Fainstein, A. Huynh, B. Perrin, B. Jusserand, A. Miard, and A. Lemaître, Phys. Rev. Lett. **99**, 217405 (2007).
[14] A. T. Hanbicki, O. M. J. van't Erve, R. Magno, G. Kioseoglou, C. H. Li, B. T. Jonker, G. Itskos, R. Mallory, M. Yasar, and A. Petrou, Appl. Phys. Lett. **82**, 4092 (2003).
[15] G. Lüpke, Surf. Sci. Rep. **35**, 75 (1999).
[16] C. Yamada and T. Kimura, Phys. Rev. B **49**, 14372 (1994).
[17] C. J. Stanton, G. D. Sanders, R. L. Liu, C. S. Kim, J. S. Yahng, E. Oh, and D. S. Kim, *Ultrafast Phenomena in Semiconductors VI*, edited by K. T. F. Tsen, J. J. Song, and H. Jiang, Vol. 4643 (SPIE, Bellingham, WA, 2002).
[18] H. Ogi, M. Fujii, N. Nakamura, T. Shagawa, and M. Hirao, Appl. Phys. Lett. **90**, 191906 (2007).
[19] W. S. Lai and X. S. Zhao, Appl. Phys. Lett. **85**, 4340 (2004).
[20] M. R. Brozel and G. E. Stillman, *Properties of Gallium Arsenide*, 3rd ed. (INSPEC, Institution of Engineering and Technology, London, United Kingdom, 1996), p. 16.